Paper:

Fabrication of Microstructures on RB-SiC by Ultrasonic Cavitation Assisted Micro-Electrical Discharge Machining

Pay Jun Liew[*,***], **Keita Shimada**[*], **Masayoshi Mizutani**[*],
Jiwang Yan[**], **and Tsunemoto Kuriyagawa**[*]

[*]Department of Mechanical Systems and Design, Tohoku University
6-6-01 Aoba, Aramaki, Aoba-ku, Sendai 980-8579, Japan
E-mail: payjun@pm.mech.tohoku.ac.jp
[**]Department of Mechanical Engineering, Faculty of Science and Technology, Keio University
3-14-1 Hiyoshi, Kohoku-ku, Yokohama 223-8522, Japan
[***]Manufacturing Process Department, Faculty of Manufacturing Engineering, Universiti Teknikal Malaysia Melaka
Hang Tuah Jaya, 76100 Durian Tunggal, Melaka, Malaysia
[Received March 31, 2013; accepted August 5, 2013]

Ultrasonic cavitation assisted micro-electrical discharge machining was used to fabricate microstructures on reaction-bonded silicon carbide. To aid the removal of debris from the machining gap and to obtain a good surface finish, carbon nanofibers were added into the dielectric fluid. The suspension of carbon nanofibers in the dielectric fluid and the cavitation bubble effect induced by the vibration of the dielectric fluid proved to be effective in reducing the deposition of tool material on the workpiece surface. The tool material deposition rate was found to be significantly affected by the vibration amplitude and the distance between the oscillator and the workpiece. With a hemispherical electrode and inclined workpiece, high accuracy micro-dimples could be obtained within a short time. A nanometer-level surface finish was successfully obtained on a hard-brittle RB-SiC mold material.

1. Introduction

In recent years, the industrial demand for microstructures such as micro-dimple arrays, micro-pyramid arrays and micro-prism arrays has been increasing. Because of the wide range of applications of these functional microstructures in optical, biomedical engineering, and microelectromechanical systems, precision manufacturing processes have become essential to produce these microstructured surfaces, not only in terms of their dimensions and shape, but also in terms of the quality of the machined surface [1].

There are many different fabrication methods for producing microstructures, such as photolithography [2], laser machining [3], dry etching [4], and a hybrid process that includes ultraviolet lithography, photoresist reflow processing, electroplating and a hot embossing technique [5]. Micro mechanical machining processes also have been used to fabricate micro-functional surface on metal and ceramic surfaces. A typical example is the use of tungsten carbide micro-endmills as micro-cutting tools [6–7]. However, commercial micro-endmills with small diameters are easily fractured, and it is difficult to detect tool wear and fracture [6]. As an alternative approach, Zhang et al. [8] used a polycrystalline diamond micro-endmill to fabricate micro-dimple arrays on a tungsten carbide workpiece.

Recently, micro-electro discharge machining has received attention from researchers as a precision machining tool for producing micro-features, such as in the fabrication of micro-molds for plastic and glass lenses. The growing popularity of micro-electrical discharge machining can be attributed to its advantages, which include low installation cost and its ability to machine complex three-dimensional shapes easily regardless of the material's hardness [9]. Furthermore, during machining with micro- electrical discharge machining, there is no direct contact between the electrode and the workpiece, which eliminates mechanical stress, chatter, and vibration problems [10].

However, to obtain microstructures with a good surface finish and high form accuracy in reaction-bonded silicon carbide (RB-SiC), the use of micro- electrical discharge machining is still a challenging issue because of its low conductivity. The deposition of the tool material on the workpiece surface not only causes surface contamination, but also deteriorates the surface finish of the workpiece [11]. To remove the debris from the machining zone, previous researchers have attempted to use a wide range of different vibration-assisted methods for micro- electrical discharge machining, such as the ultrasonic vibration of the workpiece [12–13] and a dielectric fluid [14]. In a recent paper [15], we developed a hy-

brid micro- electrical discharge machining process using a combination of ultrasonic cavitation and the addition of carbon nanofiber to the dielectric fluid. We found that this hybrid process not only improved the machining efficiency, form accuracy, and surface finish of a micro-hole, but also increased the material removal rate and machining stability of RB-SiC. Because of the limited conductivity of the RB-SiC mold material, carbon nanofibers play an important role in the process. The excellent electrical conductivity of carbon nanofiber not only improves the electro discharge frequency, material removal rate, and spark gap, but also reduces the electrode wear and electrode tip concavity. Furthermore, with the addition of carbon nanofibers, the tungsten tool material deposition can also be reduced compared to that obtained using only pure EDM oil [11, 16]. Therefore, in the present work, we attempted to use this hybrid process, to suppress the tool material deposition during the fine finishing of microstructures by using EDM. The effect of tool shape and time controlling strategies for this fine finishing were experimentally investigated.

2. Experimental Methods

2.1. Equipment and Materials

The experiments were conducted on a standard micro-electrical discharge machining machine (Panasonic MG-ED82W). This machine has a Resistor-Capacitor (RC) discharge circuit, and enables both micro wire EDM and micro die sinking machining. The discharging energy can be changed by adjusting the voltage (0 – 110 V), and/or the electrical capacitance of the RC circuit. The electrical capacitance is determined by condensers C1 – C4, which possess capacitance of 3300, 220, 100 and 10 pF, respectively. The stray capacitance of the circuit (C0) is approximately 1 pF. An ultrasonic vibration device, the SC–450 cavitation generator (Taga Electric Co., Ltd, Japan) with a power output of 50 W was used in this experiment. It has a vibration frequency of 20 kHz and a maximum amplitude of 14 μm. During the EDM process, the tool electrode was inserted through a small hole into the end of the oscillator horn of the cavitation generator. Ultrasonic vibration was applied to the dielectric fluids by the oscillator horn, which caused the cavitation effect. The workpiece material used in the experiments was RB-SiC, an important ceramic material that has a high electrical resistivity ($\sim$ 1453 Ωcm). RB-SiC is a promising material for fabricating the molding dies used in a glass molding press. The as-received sample was produced by Japan Fine Ceramics Co., Ltd. Some of the typical material properties of the sample are listed in **Table 1**. Tungsten was used as tool electrode because of its high melting point and low tool wear. Commercially available EDM oil, Casty Lube EDS (Nikko Casty Co., Ltd.), was used as the dielectric fluid. To improve the discharge frequency, 0.06 g/L of high conductivity carbon nanofibers measuring 150 nm in diameter and 6 – 8 μm in length were used as additives.

Table 1. Material properties of RB-SiC (workpiece) [17].

Properties	Values
Grain size (μm)	<1
Volume (%)	Si-12, SiC-88
Density ρ (g/cm^3)	3.12
Softening temperature (°C)	1375
Electrical resistivity (Ωcm)	~1453
Young modulus E (GPa)	407
Vickers hardness (GPa)	25–35
Thermal conductivity (W/m.K)	143

Table 2. Experimental conditions for fabrication of micro tool electrodes.

Tool electrode material	Tungsten		
Polarity	Positive (tool)	Negative (workpiece)	
Tool electrode rotational speed (rpm)	3000		
Wire/block electrode material	Brass		
	Roughing	**Semi-finishing**	**Finishing**
Voltage (V)	−110	−80	−70
Capacitance (pF)	3300	10	1

2.2. Fabrication of Micro-Tool Electrode

In preliminary work, the effects of different geometry micro-tool electrodes on the form accuracy were ascertained without using ultrasonic cavitation. Tungsten rods were shaped into rectangular, square, and triangular shapes using a block electrode method, and into a hemispherical shape using Wire Electro-Discharge Grinding (WEDG). It was presumed that these polygonal electrodes would make it easier to flush out the debris from the side gap of the working zone when electrode rotation was applied, which would help to increase the form accuracy of a micro-dimple. **Table 2** lists the experimental conditions for fabricating the tungsten tool into the desired shape, from rough machining to fine finishing. During the tool fabrication, the tungsten tool electrode was set as the anode and the block electrode/wire was set as the cathode. In the block electrode method, a conductive brass block
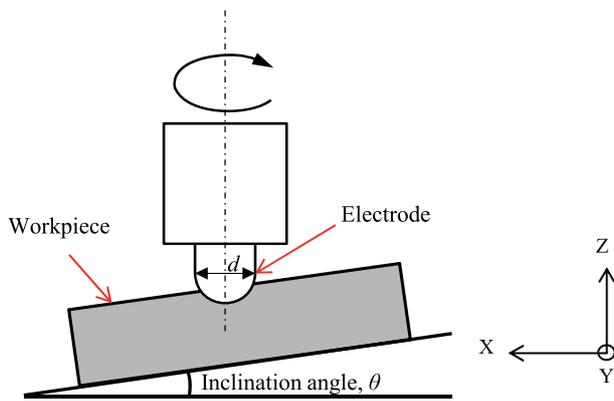
Fig. 1. Experimental setup using inclined workpiece.
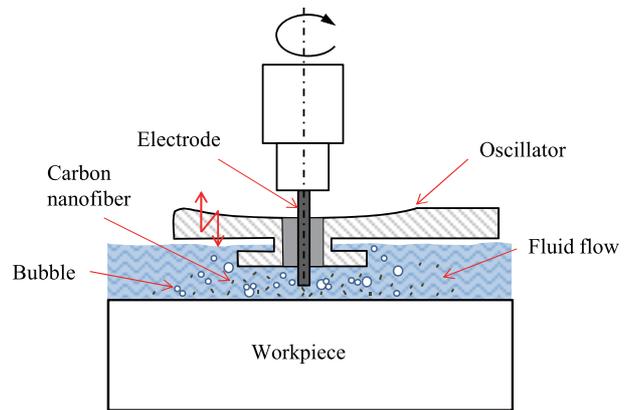
Fig. 2. Schematic diagram of ultrasonic cavitation assisted micro-electrical discharge machining experimental setup.

was selected as the tool material because of its high conductivity and high wear resistance. This method was similar to that described by Ravi and Han [18] and Perveen et al. [19]. For WEDG, a brass wire electrode was continuously fed on the guide, and the tungsten workpiece was moved perpendicularly to the wire in the Z and X directions, at a rotational speed of 3000 rpm.

2.3. Micro-Dimple Machining

First, the tungsten tools shaped by the procedure explained in the preceding section were used to machine micro-dimples on RB-SiC. Using die sinking EDM, each test was run for a 5 min, during which a negative electrode polarity was used. The effect of the machining time on the fine finishing was experimentally investigated. During the machining, the dielectric fluid was ejected through a nozzle to the machining area (external side flushing) to enhance the flushing of debris. The workpiece was set at a 10° angle, as schematically shown in **Fig. 1**. It was expected that the slight incline of the workpiece would contribute to the smooth exclusion of tungsten debris, and in turn, result in a better surface finish.

Thereafter, a combination of ultrasonic cavitation and carbon nanofibers [15] was used to control the tool material deposition on the RB-SiC machined surface. **Fig. 2** shows a schematic diagram of the experimental setup. The vibration amplitudes and distance between the oscillator and the workpiece were changed, and the extent of material migrations from the tool electrode to the RB-SiC workpiece was investigated experimentally. Each micro-electrical discharge machining test was performed on a sample for a duration of 3 min.

All of the experiments were repeated three times with newly fabricated tool electrodes, which rotated at a rotational speed of 3000 rpm during the machining of the dimples. Subsequently, the optimal conditions to improve the form accuracy and finished surface topography were used to fabricate a micro-dimple array. The experimental conditions are summarized in **Table 3**.

Table 3. Experimental conditions.

Workpiece material	RB-SiC
Electrode material	Tungsten
Polarity	Positive (workpiece) Negative (tool)
Rotational speed (rpm)	3000
Feed rate (µm/s)	3
Voltage (V)	100, 80
Condenser capacitance (pF)	3300, Stray capacitance (~1)
Electrode shape	Rectangular, hemispherical, square, triangular
Vibration frequency (kHz)	20±1.5
Vibration amplitude (µm)	0~14 (0~100%)
Working distance (mm)	1~4
Dielectric fluid	EDM oil (CASTY-LUBE EDS)
Finishing time (s)	10, 50, 70

2.4. Surface Characterization

The surface roughness of the workpiece after the EDM tests was measured using a non-contact laser probe profilometer NH-3SP (Mitaka Kouki Co. Ltd.). The EDM fabricated micro-dimples were then examined by a Scanning Electron Microscope (SEM), SU1510 (Hitachi, Co., Ltd.). Subsequently, an Energy Dispersive X-ray (EDX) analysis was used to detect material migration and to measure the amount of migrated material.
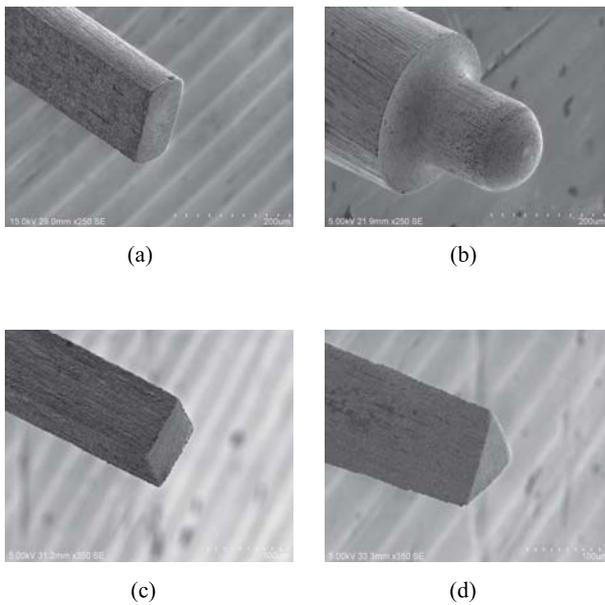
Fig. 3. Microelectrodes with different geometries: (a) rectangular, (b) hemispherical, (c) square, and (d) triangular.

Fig. 4. Micro-dimple machined at 80 V, stray capacitance using different geometry micro tool electrodes: (a) rectangular, (b) hemispherical, (c) square, and (d) triangular.

3. Results and Discussion

3.1. Effect of Tool Shape

Figure 3 shows SEM micrographs of the tungsten tool electrodes with different geometries, which were fabricated by using the procedures described in section 2.2. Electrodes of exactly the same size should be used in such experiments to allow a comparison of machining results. However, it is difficult to do this in practice. Therefore, electrodes with diameters between $\phi 90$ and $\phi 150$ μm were used in this study.

Without ultrasonic cavitation, micro-dimples were machined on the RB-SiC workpiece using the fabricated microelectrodes. The fine finishing parameters were set to 80 V and stray capacitance (~ 1 pF). The machining was performed for a constant machining time of 5 min. **Fig. 4** shows the SEM micrographs of the machined micro-dimples that were obtained with an inclined workpiece. It is clear that none of the dimples show good form accuracy, and that a cone-shaped protrusion was formed at the center of each micro-dimple. In addition, the micro-dimples that were fabricated by the rectangular, square, and triangular electrodes show concentric rings inside the dimples. This is assumed to be because of nonuniform wear of the flat-head electrode tip, which might have been caused by long machining time. During fine finishing at a low voltage, the gap between the tool and the workpiece is very small. Therefore, the electrical discharge-induced tungsten debris cannot be effectively removed from the gap by using a flat-head electrode; instead, the debris is deposited on the machined surface and/or interacts with the tool electrode [20], causing nonuniform wear of the tool tip. In contrast, the hemispherical electrode, which was non-flat head electrode, could produce better form accuracy without concentric rings inside the micro-dimple.

Thus, the next section describes step-by-step machining (from rough to fine finishing) that was conducted to control the form accuracy of the micro-dimples by using a hemispherical electrode.

3.2. Effect of Machining Time on Fine Finishing

To obtain micro-dimples with high form accuracy, step-by-step machining (from rough to fine finishing) was carried out using an inclined workpiece. Roughing regimes use a high pulse energy to remove the bulk of the material in the minimum amount of time. Semifinishing and finishing regimes use low-energy relaxation pulses to achieve a good surface finish and accurate geometry [21]. First, the micro-dimple shape was formed by a hemispherical electrode using roughing parameters (voltage 100 V, capacitance 3300 pF). It was then finished under finishing conditions (voltage 80 V, stray capacitance ~ 1 pF).

A time-controlling method was used for the fine machining to determine the optimum machining time to obtain good form accuracy. The tool electrode was fed in the Z direction, and the machining was performed for the specified time duration. The recording of machining time commenced when the first discharge was detected by the micro-electrical discharge machining, from the 0.0-μm point (starting point). The results are shown in **Fig. 5**. It is seen that a thick layer of resolidified material, induced by a high discharge energy, was not sufficiently removed with machining times of 10 (**Fig. 5(a)**) and 50 s (**Fig. 5(b)**). In contrast, after initial shape generation by rough machining a very good form accuracy without a cone-shaped protrusion could be obtained with a fine finishing time of 70 s (optimum) (**Fig. 5(c)**).
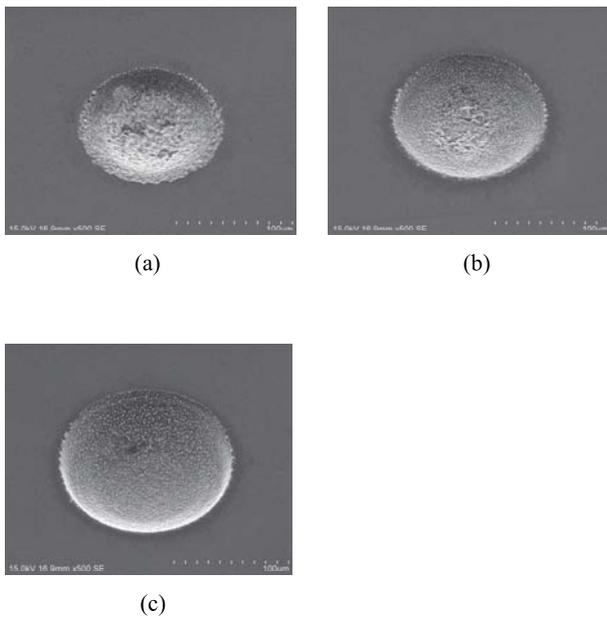
Fig. 5. Micro-dimples finished with different machining times: (a) 10 s, (b) 50 s, and (c) 70 s.

Tungsten particles
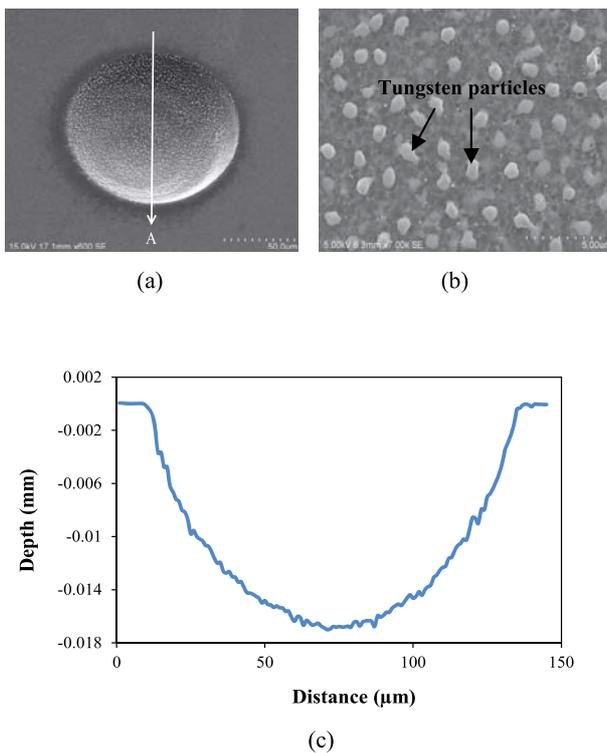
Fig. 6. SEM micrograph of micro-dimple: (a) general view, (b) detailed view of dimple surface, and (c) cross-sectional profile of machined micro-dimple along direction A in (a).

By using the aforementioned method, a micro-dimple was machined on RB-SiC, as shown in **Fig. 6(a)**. **Fig. 6(c)** shows a cross-sectional profile of the dimple, which was measured along direction A in **Fig. 6(a)**. It can be seen that a good form accuracy without a cone-shaped protru-
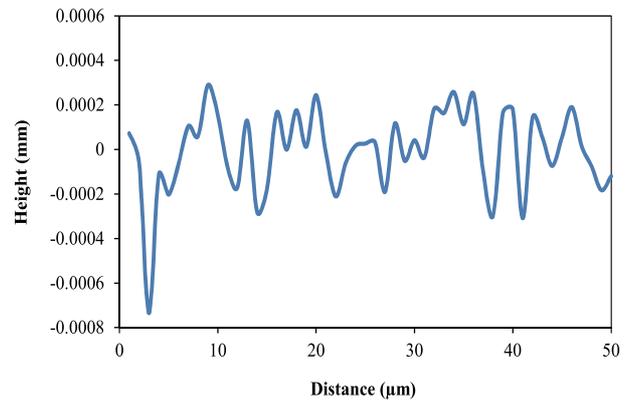
Fig. 7. Surface roughness profile of micro-dimple in **Fig. 6(a)**.

sion could be obtained with an inclined workpiece. However, as explained in [11], tungsten electrode material was found to be deposited on the machined surface, as micro-particles in an amorphous structure inside surface craters, and as a thin interdiffusion layer with a poly-crystalline structure on flat surface regions, as shown in **Fig. 6(b)**. As a result, the surface roughness increased, which deteriorated the surface integrity of the micro-dimple. To further confirm the surface roughness of the machined surface, measurement was performed using a laser-probe profiling system. The evaluation length was 50 μm, across the center of the micro-dimple along the radial direction. **Fig. 7** shows a surface profile corresponding to the micro-dimple shown in **Fig. 6(a)**. This observation was in good agreement with the microstructure observation, where the finished surface was quite rough, with a surface roughness of 0.1410 μmRa. This indicates that without ultrasonic cavitation, the step-by-step machining with an optimized finishing time on an inclined surface is helpful in obtaining good form accuracy; however, it cannot prevent electrode material deposition on the machined surface.

3.3. Effect of Vibration Amplitude

Next, to suppress the deposition of tungsten particles, ultrasonic cavitation assisted micro-electrical discharge machining with the addition of carbon nanofibers in the dielectric fluid, as explained in the previous work [15], was conducted on RB-SiC. **Fig. 8** shows SEM micrographs of machined RB-SiC surfaces obtained using different vibration amplitudes, ranging from 0 to 100%. When ultrasonic cavitation was not used, the quantity of the deposited tungsten particles was high, as shown in **Fig. 8(a)**. However, as the amplitude increased (100%, $\sim$ 14 μm), there was a rapid decrease in the amount of deposited tungsten particles, as shown in **Fig. 8(d)**. To further confirm the deposited tungsten elemental composition, the machined surface was analyzed using EDX. **Fig. 9** shows the changes in tungsten weight percentage with amplitude. It can be seen that the weight percentage of the deposited tungsten material decreases significantly as the amplitude increases.

(a)

(b)

(c)

(d)
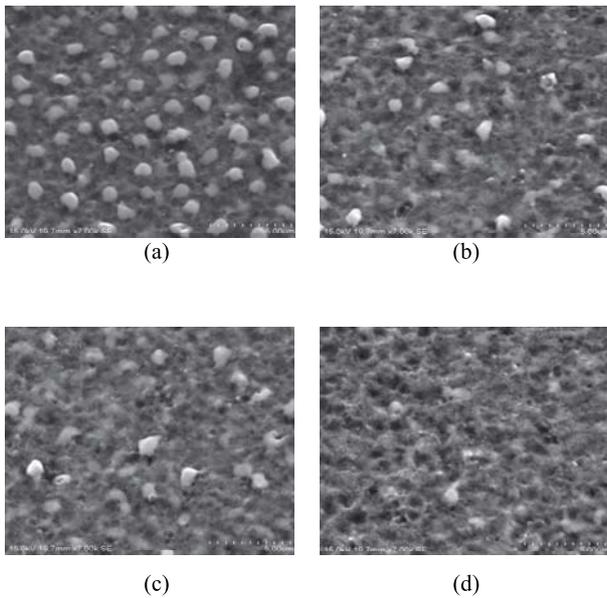
Fig. 8. Machined surface at 80 V and stray C, but with different levels of vibration amplitude and carbon nanofiber addition: (a) without ultrasonic cavitation, (b) 20%, (c) 60%, and (d) 100%.

(a)

(b)

(c)

(d)

Fig. 10. Machined surfaces at 80 V and stray C but with different working distances: (a) 1 mm, (b) 2 mm, (c) 3 mm, and (d) 4 mm.

Fig. 9. Effect of vibration amplitude on weight percentage of deposited tungsten electrode material.

According to Vyas and Preece [22], at an extremely low vibration amplitude, the acoustic intensity is insufficient to produce cavitation, which makes it difficult to remove the debris from the working area. As the amplitude of the vibration increases, even though the number of bubbles increases, the formation of cloud cavitation is still marginal and insufficient to flush out the debris to a significant degree. Consequently, unremoved debris remains on the machined surface, as shown in **Figs. 8(b)** and **(c)**. At a critical amplitude (in this case, 14 μm), the number of bubbles increases significantly [22], and as a result of the pressure fluctuation that is induced by the ultrasonic waves, the generated cloud cavitation tends to oscillate rapidly at the working area, as explained in [15]. Therefore, the electrical discharge-induced tungsten debris can be effectively removed from the narrow gap through cloud

cavitation, resulting in a better surface finish with minimum deposition of tungsten particles. On the basis of these results, we can say that it is important to increase the vibration amplitude to suppress the tungsten material deposition. In this study, the optimal value of vibration amplitude was 100%, which was around 14 μm.

3.4. Effect of Working Distance

The effect of the working distance on the deposition of tungsten tool material on the machined surface was investigated. The results are shown in **Fig. 10**. The working distance in this context means the distance between the oscillator and the workpiece during the EDM process. The working distance ranged from 1 to 4 mm at a constant amplitude of 14 μm (100%). It is seen that the quantity of the deposited particles increases when a longer working distance is used, as shown in **Fig. 10(d)**. In contrast, a short working distance contributed to a significant reduction in the deposited tungsten particles (**Fig. 10(a)**). Presumably, when the working distance was longer, the cloud cavitation was not strong enough to reach the working area. Hence, the tungsten debris could not be removed significantly, and instead, deposited on the machined surface.

On the other hand, when the oscillator was placed closer to the workpiece, the generated cloud cavitation oscillated rapidly at the working area and easily flushed the tungsten debris out of the working area. This condition was considered to be helpful to provide the desired flushing. Thus, a smoother surface with minimum deposition of tungsten particles could be obtained.

3.5. Fabrication of Micro-Dimple Array

Using the optimum machining conditions obtained in the previous sections, a micro-dimple array was fabricated on the RB-SiC mold material. **Fig. 11(a)** shows an SEM micrograph of a single dimple. Good form accuracy without a cone-shaped protrusion was obtained using the fine finishing conditions of 80 V and stray capacitance. **Fig. 11(b)** shows a magnified view of the dimple surface. Clearly, the adherence of tungsten particles could be significantly suppressed by the combination of ultrasonic cavitation and carbon nanofibers, where the amount of deposited tungsten micro particles was minimal. The surface roughness was measured across the center of the micro-dimple, and the evaluation length was 50 μm. The surface profile is shown in **Fig. 11(d)**. It should be noted that the surface roughness of the micro-dimple improved significantly, and a nanometer-level surface roughness (78.1 nmRa) could be obtained. The finished surface was far smoother than that in **Fig. 6**. **Fig. 11(c)** shows an SEM micrograph of a fabricated micro-dimple array. This result demonstrated that the ultrasonic cavitation assisted micro-electrical discharge machining with the addition of carbon nanofibers in the dielectric fluid and a slightly inclined workpiece were helpful for obtaining high form accuracy and a good surface finish on the RB-SiC machined surface, provided a suitable machining time was used for the fine finishing.

4. Conclusion

Ultrasonic cavitation assisted micro-electrical discharge machining experiments were performed with the addition of carbon nanofibers in the dielectric fluid. The effects of the vibration amplitude, working distance, electrode shape and machining time were investigated. The following conclusions were drawn:

1. Ultrasonic cavitation assisted micro-electrical discharge machining with carbon nanofibers added to the dielectric fluid can significantly reduce the deposition of tool material on the workpiece surface, which in turn, improves the surface finish of the machined surface.

2. The vibration amplitude is closely related to the deposition of the tool material, with a higher amplitude resulting in a lower deposition rate.

3. Decreasing the distance between the oscillator and the workpiece is helpful in preventing the deposition of the tool material.

4. Neglecting the cone-shaped protrusions, hemispherical tools produce better form accuracy without concentric rings inside the micro-dimple as compared to other microelectrode shapes.

5. With an inclined workpiece and suitable fine-finishing time ($\sim$ 70 s), high form accuracy could be obtained for a micro-dimple.

(a)
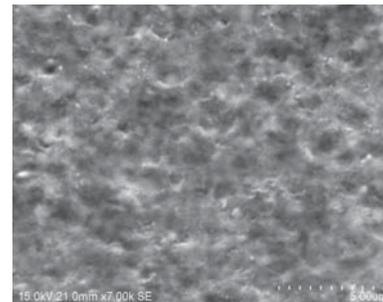
(b)

(c)
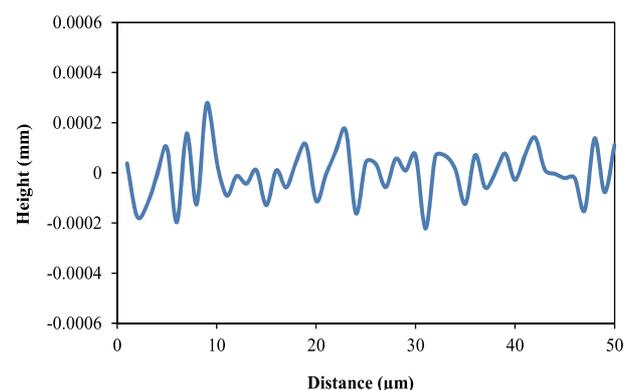
(d)

Fig. 11. SEM micrographs of machined micro-dimples: (a) single dimple, (b) magnified view of dimple surface, (c) dimple array (3×1), and (d) surface roughness profile of (a).

6. Under the optimized conditions, a micro-dimple array with high form accuracy and a nanometer-level surface finish was successfully fabricated.

References:

[1] J. C. Hung, J. K. Lin, B. H. Yan, H. S. Liu, and P. H. Ho, "Using a helical micro-tool in micro-EDM combined with ultrasonic vibration for micro-hole machining," J. of Micromechanics and Microengineering, Vol.16, pp. 2705-2713, 2006.

[2] M. H. Wu and G. M. Whitesides, "Fabrication of two-dimensional arrays of microlenses and their applications in photolithography," J. of Micromechanics and Microengineering, Vol.12, pp. 747-758, 2002.

[3] C. C. Chiu and Y. C. Lee, "Fabricating of aspheric micro-lens array by excimer laser micromachining," Optics and Lasers in Engineering, Vol.49, pp. 1232-1237, 2011.

[4] M. B. Stern and T. R. Jay, "Dry etching for coherent refractive microlens arrays," Optical Engineering, Vol.33, No.11, pp. 3547-3551, 1994.

[5] C. T. Pan and C. H. Su, "Fabrication of gapless triangular microlens array," Sensors and Actuators A, Vol.134, pp. 631-640, 2007.

[6] I. S. Kang, J. S. Kim, M. C. Kang, and K. Y. Lee, "Tool condition and machined surface monitoring for micro-lens array fabrication in mechanical machining," J. of Materials Processing Technology, Vol.201, pp. 585-589, 2008.

[7] H. Weule, V. Huntrup, and H. Tritschler, "Micro-cutting of steel to meet new requirements in miniaturization," CIRP Annals-Manufacturing Technology, Vol.50, pp. 61-64, 2001.

[8] Z. Zhang, H. Peng, and J. Yan, "Micro-cutting characteristics of EDM fabricated high-precision polycrystalline diamond tools," Int. J. of Machine Tools and Manufacture, Vol.65, pp. 99-106, 2013.

[9] D. Reynaerts, W. Meeusen, and H. V. Brussel, "Machining of three-dimensional microstructures in silicon by electro-discharge machining," Sensors and Actuators A, Vol.67, pp. 159-165, 1998.

[10] K. H. Ho and S. T. Newman, "State of the art electrical discharge machining (EDM)," Int J. of Machine Tools and Manufacture, Vol.43, pp. 1287-1300, 2003.

[11] P. J. Liew, J. Yan, and T. Kuriyagawa, "Experimental investigation on material migration phenomena in micro-EDM of reaction-bonded silicon carbide," Applied Surface Science, Vol.276, pp. 731-743, 2013.

[12] R. Garn, A. Schubert, and H. Zeidler, "Analysis of the effect of vibrations on the micro-EDM process at the workpiece surface," Precision Engineering, Vol.35, pp. 364-368, 2011.

[13] K. T. Hoang and S. H. Yang, "A study on the effect of different vibration-assisted methods in micro-WEDM," J. of Materials Processing Technology, Vol.213, pp. 1616-1622, 2013.

[14] T. Ichikawa and W. Natsu, "Realization of micro-EDM under ultra-small discharge energy by applying ultrasonic vibration to machining fluid," Procedia CIRP, Vol.6, pp. 326-331, 2013.

[15] P. J. Liew, J. Yan, and T. Kuriyagawa, "Fabrication of micro deep holes on reaction-bonded SiC by ultrasonic cavitation assisted micro EDM," Int. J. of Machine Tools and Manufacture. (In press)

[16] P. J. Liew, J. Yan, and T. Kuriyagawa, "Carbon nanofiber assisted micro electro discharge machining of reaction-bonded silicon carbide," J. of Materials Processing Technology, Vol.213, Issue 7, pp. 1076-1087, 2013.

[17] Technical data provided by the manufacture of the workpiece material.

[18] N. Ravi and H. Huang, "Fabrication of symmetrical section microfeatures using the electro-discharge machining block electrode method," J. of Micromechanics and Microengineering, Vol.12, pp. 905-910, 2002.

[19] A. Perveen, Y. S. Wong, and M. Rahman, "Fabrication of different geometry cutting tools and their effect on the vertical micro-grinding of BK7 glass," Int. J. of Advanced Manufacturing Technology, Vol.61, pp. 101-115, 2012.

[20] B. Ekmekci and A. Sayar, "Debris and consequences in micro electric discharge machining of micro-holes," Int. J. of Machine Tools and Manufacture, Vol.65, pp. 58-67, 2013.

[21] S. Clijsters, K. Liu, D. Reynaerts, and B. Lauwers, "EDM technology and strategy development for the manufacturing of complex parts in SiSiC," J. of Materials Processing Technology, Vol.210, pp. 631-641, 2010.

[22] B. Vyas and C. M. Preece, "Stress produced in a solid by cavitation," J. of Applied Physics, Vol.47, No.12, pp. 5133-5138, 1976.

Name:
Pay Jun Liew

Affiliation:
Ph.D Student, Department of Mechanical Systems and Design, Graduate School of Engineering, Tohoku University

Address:
6-6-01 Aoba, Aramaki, Aoba-ku, Sendai 980-8579, Japan
Brief Biographical History:
2005- Graduated from Kolej Universiti Tun Hussein Onn, Malaysia with Bachelors of Manufacturing Engineering
2007- Graduated from Coventry University, United Kingdom with Master of Manufacturing Systems Engineering
Main Works:
● P. J. Liew, J. Yan, and T. Kuriyagawa, "Carbon nanofiber assisted micro electro discharge machining of reaction-bonded silicon carbide," J. of Materials Processing Technology, Vol.213, Issue 7, pp. 1076-1087, 2013.
● P. J. Liew, J. Yan, and T. Kuriyagawa, "Experimental investigation on material migration phenomena in micro-EDM of reaction-bonded silicon carbide," Applied Surface Science, Vol.276, pp. 731-743, 2013.
● P. J. Liew, J. Yan, T. Masaki, and T. Kuriyagawa, "Effect of different dielectric fluids on micro EDM of low conductivity ceramic material RB-SiC," Advanced Materials Research, Vol. 565, pp. 529-534, 2012.
Membership in Academic Societies:
● The Japan Society of Mechanical Engineers (JSME)

Name:
Keita Shimada

Affiliation:
Assistant Professor, Department of Mechanical
Systems and Design, Graduate School of Engi-
neering, Tohoku University

Address:
6-6-01 Aoba, Aramaki, Aoba-ku, Sendai 980-8579, Japan
Brief Biographical History:
2009- Graduated from Tohoku University, Japan with Master of
Engineering
2012- Graduated from Tohoku University, Japan with Doctor of
Engineering
2012- Assistant Professor, Department of Mechanical Systems and Design,
Tohoku University
Main Works:
● K. Shimada, N. Yoshihara, J. Yan, T. Kuriyagawa, Y. Sueish, and
H. Tezuka, "Ultrasonic-assisted Grinding of Ultra-High Purity SUS 316,"
Int. J. Automation Technology, Vol.5 No.3, pp. 427-432, 2011.
● K. Shimada, P. J. Liew, T. Zhou, J. Yan, and T. Kuriyagawa, "Statistical
Approach Optimizing Slant Feed Grinding," J. Adv. Mech. Design,
Systems and Manu. Vol.6, No.6, 2012.
Membership in Academic Societies:
● Japan Society of Mechanical Engineers (JSME)
● Japan Society for Precision Engineering (JSPE)
● Japan Society for Abrasive Technology (JSAT)

Name:
Jiwang Yan

Affiliation:
Professor, Department of Mechanical Engineer-
ing, Faculty of Science and Technology, Keio
University

Address:
3-14-1 Hiyoshi, Kohoku-ku, Yokohama 223-8522, Japan
Brief Biographical History:
2000-2001 Research Associate, Tohoku University
2001-2005 Associate Professor, Kitami Institute of Technology
2005-2012 Associate Professor, Tohoku University
2012-present Professor, Keio University
Main Works:
● Ultraprecision machining of optical and optoelectronic materials,
fabrication of micro-structured surfaces, micro/nano machining mechanics,
laser processing of material and ultraprecision molding technology
Membership in Academic Societies:
● Japan Society of Mechanical Engineers (JSME)
● Japan Society for Precision Engineering (JSPE)
● Japan Society for Abrasive Technology (JSAT)
● Japan Society for Applied Physics (JSAP)
● American Society for Precision Engineering (ASPE)
● European Society for Precision Engineering and Nanotechnology
(euspen)

Name:
Masayoshi Mizutani

Affiliation:
Associate Professor, Department of Mechanical
Systems and Design, Graduate School of Engi-
neering, Tohoku University

Address:
6-6-01 Aoba, Aramaki, Aoba-ku, Sendai 980-8579, Japan
Brief Biographical History:
2003- Completed Master Course Integrated Design Engineering, Graduate
School of Science and Technology, Keio University
2004- Junior Research Associate, Ohmori Materials Fabrication
Laboratory, RIKEN
2006- Completed Doctor Course Integrated Design Engineering, Graduate
School of Science and Technology, Keio University
2006- Collaboration Researcher, Advanced Development & Supporting
Center, RIKEN
2007- Collaboration Researcher, Ohmori Materials Fabrication Laboratory,
RIKEN
2009- Special Postdoctoral Researcher, Ohmori Materials Fabrication
Laboratory, RIKEN
2011- External Collaborative Researcher, Sophia University
2012- Collaboration Researcher, Ohmori Materials Fabrication Laboratory,
RIKEN
2012- Associate Professor, Department of Mechanical Systems and
Design, Tohoku University
Main Works:
● Micro/meso mechanical manufacturing (M4 Process), laser process,
powder jet deposition (PJD), functional interface, biomaterials,
bio-medical applications, biomimetic surface
Membership in Academic Societies:
● Japan Society of Mechanical Engineers (JSME)
● Japan Society for Precision Engineering (JSPE)
● Japan Society for Abrasive Technology (JSAT)

Name:
Tsunemoto Kuriyagawa

Affiliation:
Professor, Department of Mechanical Systems
and Design, Graduate School of Engineering,
Tohoku University

Address:
6-6-01 Aoba, Aramaki, Aoba-ku, Sendai 980-8579, Japan
Brief Biographical History:
1984-1990 Research Associate, Tohoku University
1990-1992 Assistant Professor, Tohoku University
1991-1992 Visiting Professor, University of Connecticut
1992-2002 Associate Professor, Tohoku University
2003-present Professor, Tohoku University
Main Works:
● Nano-precision mechanical manufacturing, micro/meso mechanical
manufacturing (M4 process), powder jet deposition, and creation of
functional interface
Membership in Academic Societies:
● Science Council of Japan (SCJ)
● International Committee for Abrasive Technology (ICAT)
● International Society for Nanomanufacturing (ISNM)
● Japan Society of Mechanical Engineers (JSME)
● Japan Society for Precision Engineering (JSPE)
● Japan Society for Abrasive Technology (JSAT)